Chapter 1

Preliminaries

Definition 1.0.1. The set $D \subset \mathbb{C}^n$ such that all points are isolated:

$$\forall\, z \in D\ \exists\, \epsilon > 0 :\ B(z, \epsilon) \cap D = \{z\}$$

is a **discrete set**. ⌟

1.1 Delone set

Delone set is such a set that is both relatively dense and uniformly discrete. These notions are defined using two parameters called packing a covering radius.

Definition 1.1.1. The **packing radius** of a set $D \subset \mathbb{C}^n$ is the number:

$$R_P = \frac{1}{2} \sup \{ r_1 \in \mathbb{R} \mid \forall\, z_1, z_2 \in D, z_1 \neq z_2 :\ \|z_1 - z_2\| > r_1 \}$$

⌟

Remark. Open balls of packing radius centered at the points of the set are disjoint.

Definition 1.1.2. The **covering radius** of a set $D \subset \mathbb{C}^n$ is the number:

$$R_C = \inf \{ r_2 > 0 \mid \forall\, z \in \mathbb{C}^n :\ B(z, r_2) \cap D \neq \emptyset \}$$

⌟

Remark. Union of closed balls of covering radius centered at the points of the set is the entire space $\mathbb{C}^n$.

Definition 1.1.3. Let $D \subset \mathbb{C}^n$.
If D has positive packing radius R_P then it is **uniformly discrete**.
If D has finite covering radius R_C then it is **relatively dense**.
If D has both positive packing radius R_P and finite covering radius R_C then it is a **Delone set**. ⌟

1.2 Voronoi diagram

Definition 1.2.1. Let $P \subset \mathbb{R}^n$ be a discrete set and $x \in P$. The **Voronoi polygon** or **Voronoi cell** or **Voronoi tile** of x on P is the set:

$$V_P(x) = \{y \in \mathbb{R}^n \,|\, \forall z \in P, z \neq x : \|y - x\| \leq \|y - z\|\}$$

Voronoi polygon $V_P(x)$ is said to **belong** to the point x and x is called the **center** of the Voronoi cell $V_P(x)$. ⌟

Remark. When there can be no confusion as to what set P is, the index P may be omitted: $V(x)$.

Definition 1.2.2. Let $P \subset \mathbb{R}^n$ be a discrete set. The **Voronoi diagram** or **Voronoi tessellation** is the set:

$$\{V(x) \,|\, x \in P\}$$

⌟

Definition 1.2.3. Let $P \subset \mathbb{R}^n$ be a discrete set. The set of centered Voronoi tiles:

$$\{V(x) - x \,|\, x \in P\}$$

is called the **list of Voronoi tiles**. ⌟

Remark. The Voronoi diagram can be viewed as an image whereas the list of Voronoi tiles can be viewed as a list of Voronoi polygon shapes.

Definition 1.2.4. Let $P \subset \mathbb{R}^n$ be a discrete set and let $x \in P$. The **radius** of the Voronoi polygon is the number:

$$\sup_{y \in V(x)} \|y - x\|$$

⌟

Definition 1.2.5. Let $P \subset \mathbb{R}^n$ be a discrete set and let $x \in P$. The set of points of P that directly shape the Voronoi polygon $V_P(x)$:

$$D_P(x) = \bigcap \left\{Q \subset P \,|\, V_Q(x) = V_P(x)\right\}$$

is called the **domain** of x or of $V_P(x)$. ⌟

It will be very useful to explore the Voronoi tessellation on a Delone set.

Theorem 1.2.1. *Let $P \subset \mathbb{R}^n$ be a Delone set with covering radius R_C and let $x \in P$. Then*

$$V(x) \subset \overline{B(x, R_C)}$$

Proof. By definition of the covering radius 1.1.2, for any point $y \in \mathbb{R}^n \setminus \overline{B(x, R_C)}$ there exists $w \in P$ such that $w \in B(y, R_C)$. Therefore w is closer to y than x and so $y \notin V(x)$. □

Theorem 1.2.2. *Let $P \subset \mathbb{R}^n$ be a Delone set with covering radius R_C and let $x \in P$. Then*

$$D(x) \subset B(x, 2R_C)$$

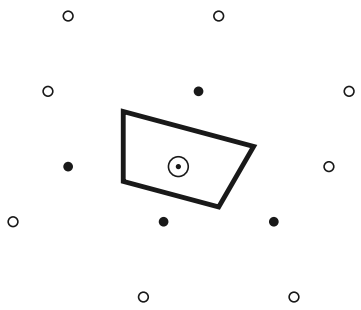

Figure 1.1: Example of Voronoi tile. The set P are all the points $\bullet$, $\circ$ and $\odot$. The polygon is the Voronoi cell belonging to the $\odot$ point. The $\bullet$ points are the domain of the Voronoi polygon (i.e. the $\circ$ points do not affect the shape of the Voronoi polygon).

Proof. If the points of the domain would be further, the Voronoi tile would not be inside $\overline{B(x, R_C)}$. □

The relationship between the Voronoi polygons and the covering radius is actually even more intricate, as the following theorem shows.

Theorem 1.2.3. *Let $P \subset \mathbb{R}^n$ be a Delone set with covering radius R_C and let $x \in P$. Then the covering radius R_C is the supremum of the radii of the Voronoi tiles:*

$$R_C = \sup_{x \in P} \left\{ \sup_{y \in V(x)} \|y - x\| \right\}$$

Proof. Let's denote the supremum of radii $r = \sup_{x \in P} \left\{ \sup_{y \in V(x)} \|y - x\| \right\}$. We have already proven that $r \leq R_C$.

Now assume that $r < R_C$. Then there is a point $y \in \mathbb{R}^n$ such that $B(y, R_C) \cap P = \emptyset$ and yet $y \in V(w)$ for some $w \in P$ and thus $\|w - y\| \leq r$. That is of course a contradiction. □

1.3 Number theory

The study of quasicrystals relies heavily on number theory. Therefore this section lists the definitions and their implications that are used further. For proofs of our claims we refer to [**?**]

Definition 1.3.1. Let $P \subset \mathbb{C}$. The ring of polynomials in x with coefficients in P is denoted by $P[x]$. ⌟

Definition 1.3.2. Polynomial $f \in \mathbb{C}[x]$ such that $f(x) = \sum_{k=0}^{m} \alpha_k x^k$ where $\alpha_m = 1$ is a **monic polynomial**. ⌟

Definition 1.3.3. Polynomial $f \in \mathbb{C}[x]$ such that $\forall\, g, h \in \mathbb{C}[x] : \; f \neq gh$ is an **irreducible polynomial**. ⌟

1.3.1 Algebraic numbers, minimal polynomial and degree

Definition 1.3.4. Let $\alpha, \beta \in \mathbb{C}$.
If there exists a monic polynomial $f \in \mathbb{Q}[x]$ such that $f(\alpha) = 0$, then α is an **algebraic number**. The set of algebraic numbers is denoted as $\mathbb{A}$.
If there exists a monic polynomial $g \in \mathbb{Z}[x]$ such that $g(\beta) = 0$, then β is an **algebraic integer**. The set of algebraic integers is denoted as $\mathbb{B}$. ⌟

Definition 1.3.5. Irreducible monic polynomial $f \in \mathbb{Q}[x]$ of the smallest degree such that $f(\alpha) = 0$ for $\alpha \in \mathbb{A}$ is the **minimal polynomial** of α. It is usually denoted as f_α. ⌟

Definition 1.3.6. The **degree** of an algebraic number is the degree of its minimal polynomial. ⌟

Remark. For each algebraic number there exists exactly one minimal polynomial.

1.3.2 Galois isomorphism

Definition 1.3.7. Let $\alpha \in \mathbb{A}$ of degree m and $f_\alpha \in \mathbb{Q}[x]$ be it's minimal polynomial. The $(m-1)$ other roots of f_α are called **conjugate roots** of α and are denoted as $\alpha^{(1)}$, $\alpha^{(2)}$, …, $\alpha^{(m-1)}$. ⌟

Remark. Consistently with the notation of its conjugate roots, α may be denoted as $\alpha^{(0)}$ or $\alpha^{(m)}$.

Remark. For low degrees the upper indexes are often written in unary – e.g. $\alpha, \alpha', \alpha''$.

Definition 1.3.8. Let $\alpha \in \mathbb{A}$ of degree m. The **extension ring** of the number α is the set:

$$\mathbb{Z}(\alpha) = \left\{ a_0 + a_1\alpha + a_2\alpha^2 + \cdots + a_{m-1}\alpha^{m-1} \mid a_i \in \mathbb{Z} \right\}$$

⌟

Definition 1.3.9. Let $\alpha \in \mathbb{A}$ of degree m. The **extension field** of the number α is the set:

$$\mathbb{Q}(\alpha) = \left\{ b_0 + b_1\alpha + b_2\alpha^2 + \cdots + b_{m-1}\alpha^{m-1} \mid b_i \in \mathbb{Q} \right\}$$

⌟

Definition 1.3.10. Let $\alpha \in \mathbb{A}$ of degree m and let $\alpha^{(1)}$, $\alpha^{(2)}$, …, $\alpha^{(m-1)}$ be its conjugate roots. Then $\mathbb{Q}(\alpha)$, $\mathbb{Q}(\alpha')$, …, $\mathbb{Q}(\alpha^{(m-1)})$ are isomorphic. The **Galois isomorphisms** are:

$$\sigma_i : \mathbb{Q}(\alpha) \to \mathbb{Q}\big(\alpha^{(i)}\big) \quad \text{induced by} \quad \sigma_i(\alpha) = \alpha^{(i)} \qquad i \in \widehat{m-1}$$

⌟

Galois isomorphisms play a significant role of the definition of the quasicrystals, so they surely deserve an example.

The Galois isomorphism σ_0 is always identity.

In general the Galois isomorphism σ_i exchanges α of degree m with its ith conjugate root.

$$\sigma_i\big(b_0 + b_1\alpha + b_2\alpha^2 + \cdots + b_{m-1}\alpha^{m-1}\big) = b_0 + b_1\alpha^{(i)} + b_2\big(\alpha^{(i)}\big)^2 + \cdots + b_{m-1}\big(\alpha^{(i)}\big)^{m-1}$$

Since further we will mostly work only with quadratic algebraic numbers (i.e. of degree 2), there will only be two roots of a given minimal polynomial and two Galois isomorphisms, namely the identity and $\sigma_1(\alpha) = \alpha'$. Moreover $\alpha' \in \mathbb{Q}(\alpha)$, thus σ_1 is an automorphism of the quadratic field $\mathbb{Q}(\alpha)$ and it is often denoted only as $'$ – i.e. $\sigma_1(x) = x'$ for $x \in \mathbb{Q}(\alpha)$.

1.3.3 Root of unity, cyclotomic polynomial

Definition 1.3.11. Every $\zeta \in \mathbb{C}$ such that $\zeta^n - 1 = 0$ for $n \in \mathbb{N}$ is called the n**th root of unity** or just **root of unity** if n is not given. Minimal $d \in \mathbb{N}$ for which $\zeta^d - 1 = 0$ is the **order** of ζ. Nontrivial root of unity is different from one. ⌟

Remark. Nontrivial root of unity is a root of polynomial $\frac{x^n-1}{x-1}$.

Remark. nth root of unity may be written as $\zeta = e^{2k\pi i/n}$ for $k \in \{0, 1, \ldots, n-1\}$.

Theorem 1.3.1. *Degree of nth root of unity ζ is $\varphi(n)$, where φ is the Euler function.*

Now we would like to look at the Galois isomorphisms of nth root of unity ζ of degree 4. It will be evident why 4 later. In accordance to the previous theorem, that means $\varphi(n) = 4$.

The three conjugate roots of ζ are also nth roots of unity and as such they are powers of ζ, specifically $\{\zeta^k | k \perp n, k > 1\}$.

Since $k \perp n$ implies $(n-k) \perp n$ and also

$$\cos\left(\frac{2k\pi}{n}\right) = \cos\left(\frac{2\,(n-k)\,\pi}{n}\right) \quad \text{and} \quad \sin\left(\frac{2k\pi}{n}\right) = -\sin\left(\frac{2\,(n-k)\,\pi}{n}\right)$$

the four roots $\zeta^{(0)}, \zeta^{(1)}, \zeta^{(2)}, \zeta^{(3)}$ appear in pairs of complex conjugates. Therefore among the four Galois isomorphisms there are two that do not change the real part of ζ and two that do change it. This will become very significant once we introduce the Pisot-cyclotomic numbers.

1.3.4 Pisot numbers

Definition 1.3.12. Let $\beta \in \mathbb{B}$ be an algebraic integer of degree m, $\beta > 1$ and for all conjugate roots β', β'', $\ldots$, $\beta^{(m-1)}$ it holds

$$|\beta^{(i)}| < 1 \qquad \forall\, i \in \widehat{m-1}$$

Then β is called **Pisot** number. ⌟

As we will see in Section 2.2, Pisot numbers represent another crucial notion to our quasicrystal model.

1.3.5 Vieta's formulas

Since we will work a lot with roots of quadratic equations we want to, just for completeness, show the Vieta's formulas in the form that we will use them.

The roots $x, x' \in \mathbb{C}$ of quadratic polynomial $ax^2 + bx + c$ satisfy:

$$x + x' = -\frac{b}{a} \qquad \text{and} \qquad xx' = \frac{c}{a}$$

For a monic quadratic polynomial ($a = 1$) we have:

$$x + x' = -b \qquad \text{and} \qquad xx' = c$$

Lastly since we are interested in expressing one root in terms of the other:

$$x = -b - x' \qquad \text{and} \qquad x = \frac{c}{x'}$$

1.4 Crystallography

Even though we are further going to work only with quasicrystals, they are often described by their differences from crystals.

A lattice is usually used as a model for a crystal.

Definition 1.4.1. Let $\{\mathbf{e}_1, \ldots, \mathbf{e}_d\}$ be a basis of $\mathbb{R}^d$ for $d \in \mathbb{N}$. **Lattice** in $\mathbb{R}^d$ is the set

$$L = \bigoplus_{j=1}^{d} \mathbb{Z}\,\mathbf{e}_j$$

⌟

There is an important theorem in crystallography, the crystallographic restriction theorem, that limits the rotational symmetries available to crystals. Here we only show the two dimensional variant.

Theorem 1.4.1. *Two dimensional lattices are limited to 2-fold, 3-fold, 4-fold, and 6-fold rotational symmetries.*

These rotational symmetries, 2-fold, 3-fold, 4-fold, and 6-fold, are thus referred to as **crystallographic** rotational symmetries.

Quasicrystals are of course not bounded by the crystallographic restriction theorem and therefore have different rotational symmetries, we will refer to different rotational symmetries as **non-crystallographic**.

1.5 Cut-and-project scheme

We are using cut-and-project scheme to model the quasicrystals. Here is a brief introduction into its workings.

In general, cut-and-project is a specific way of selecting a subset from a larger set.

The cut-and-project scheme utilizes $m + n$ dimensional lattice $L \subset \mathbb{R}^{m+n}$, m dimensional subspace $V_1 \subset \mathbb{R}^{m+n}$ and n dimensional subspace $V_2 \subset \mathbb{R}^{m+n}$.

Further we define two projections $\pi_1 : \mathbb{R}^{m+n} \to V_1$ and $\pi_2 : \mathbb{R}^{m+n} \to V_2$ such that $\pi_1|_L$ is injection and $\pi_2(L)$ is dense in V_2.

These projections are where the 'project' part of the cut-and-project scheme comes from. The 'cut' part comes from a bounded subset $\Omega \subset V_2$ with nonempty interior usually referred to as **window**.

All put together the cut-and-project scheme produces a subset $Q \subset \pi_1(L)$:

$$Q = \{\pi_1(x) \mid \pi_2(x) \in \Omega,\, x \in L\}$$

Put in words the set Q are π_1 projections of those points of L whose π_2 projections fit in the window Ω.

The notation can be somewhat simplified by composing a projection between $\pi_1(L)$ and $\pi_2(L) - \pi_2 \circ \pi_1^{-1}$, usually denoted as $*$ and referred to as a **star map**. Q then becomes:

$$Q = \{x \in V_1 \mid x^* \in \Omega\}$$

This is the form in which we will use the cut-and-project scheme.

Chapter 2

Quasicrystal

2.1 Quasicrystal

Unfortunately, there is so far no established mathematical definition of a quasicrystal, in the most basic terms it is just a set that is ordered but not periodic.

We are going to introduce our own attributes that a set $\Lambda \subset \mathbb{C}$ needs to have to be a quasicrystal.

First we require Λ to be not too dense but also not too discrete. In other words to have uniform discreetness as well as finite density.

1. uniform discreteness:

$$\exists\, r_1 > 0,\ \forall z_1, z_2 \in \Lambda, z_1 \neq z_2 :\ |z_1 - z_2| > r_1$$

2. relative density:

$$\exists\, r_2 > 0,\ \forall z \in \mathbb{C} :\ B(z, r_2) \cap \Lambda \neq \emptyset$$

Next we want finite local complexity. Sometimes this attribute is written as finiteness of a set of intersections of Λ with balls centered at any point in $\mathbb{C}$ of fixed but arbitrary radius:

$$\forall\, \rho > 0 :\ \big|\{\Lambda \cap B(x, \rho) \mid \forall x \in \Lambda\}\big| < \infty$$

However since we are going to study the Voronoi diagram of Λ we directly require the list of Voronoi tiles of Λ to be finite.

3. finite local complexity:

$$\big|\{V(x) - x \,|\, x \in \Lambda\}\big| < \infty$$

So far we have achieved the orderedness part but even periodic lattices have these properties. To break the periodicity we are going to require non-crystallographic rotational symmetry and nontrivial dilation.

4. rotational symmetry:

$$\exists\, \zeta = e^{2\pi i/n},\ n \notin \{2, 3, 4, 6\} :\ \zeta\Lambda = \Lambda$$

5. dilation:

$$\exists\, \beta \in \mathbb{R} \setminus \{-1, 1\} :\ \beta\Lambda \subset \Lambda$$

It stems form these properties alone, that among other constants a quasicrystal is linked to a root of unity ζ and to a number $\beta \in \mathbb{R} \setminus \{-1, 1\}$. Of course not every pair (ζ, β) is associated with a quasicrystal.

In the next section we will go through which numbers are associated with a quasicrystal and where do they come from.

2.2 Pisot-cyclotomic numbers

Pisot-cyclotomic numbers are Pisot and are algebraically related to roots of unity. We will use these numbers in place of β from previous section.

Definition 2.2.1. Let $\rho = 2\cos(2\pi/n)$ for a given $n > 4$, its extension ring $\mathbb{Z}[\rho]$ and m order of ρ. A **Pisot-cyclotomic** number of degree m, of order n associated to ρ is a Pisot number $\beta \in \mathbb{Z}[\rho]$ such that

$$\mathbb{Z}[\beta] = \mathbb{Z}[\rho]$$

⌟

Nontrivial nth root of unity $\zeta = e^{2\pi i/n}$ is by definition a solution to equation

$$\frac{\zeta^n - 1}{\zeta - 1} = \zeta^{n-1} + \zeta^{n-2} + \cdots + \zeta + 1 = 0$$

further for $\rho = 2\cos(2\pi/n)$ it holds

$$\rho = \zeta + \bar{\zeta} \quad \Rightarrow \quad \zeta^2 = \rho\zeta - 1$$

Therefore for extension rings $\mathbb{Z}[\zeta]$ and $\mathbb{Z}[\rho]$ we have

$$\mathbb{Z}[\zeta] = \mathbb{Z}[\rho] + \mathbb{Z}[\rho]\,\zeta$$

and finally for Pisot-cyclotomic β associated to ρ we acquire

$$\mathbb{Z}[\zeta] = \mathbb{Z}[\beta] + \mathbb{Z}[\beta]\,\zeta$$

Such countable ring is of course n-fold rotationally invariant

$$\zeta^k \mathbb{Z}[\zeta] \subset \mathbb{Z}[\zeta] \qquad k \in \widehat{n-1}$$

To summarize β is real and a Pisot and it can be used to decompose n-fold rotationally invariant complex ring $\mathbb{Z}[\zeta]$ as $\mathbb{Z}[\beta] + \mathbb{Z}[\beta]\,\zeta$.

For further work we will need actual values of Pisot-cyclotomic numbers and so in the next section we will show a method for finding quadratic Pisot-cyclotomic numbers, whose quasicrystals we will later analyze. The method could of course be generalized to different degrees.

2.2.1 Quadratic Pisot-cyclotomic numbers

Remark. Even though we are mainly focusing on two dimensional quasicrystals, that is not dictated by the quadratic-ness of β. Quadratic Pisot-cyclotomic numbers are also associated to arbitrarily dimensional quasicrystals.

As stated in preliminaries, the degree of root of unity of order n is $\varphi(n)$ (where φ is the Euler function). From the decomposition in the previous section we can easily infer that the degree of ζ is double of degree of β (or ρ). Moreover we are looking for β of degree 2. Together we acquire the following equation.

$$\varphi(n) = 2 \cdot 2 = 4$$

With help from the Euler product formula we can show that such equation holds only for $n \in \{5, 8, 10, 12\}$.

For each $n \in \{5, 8, 10, 12\}$ there is $\rho = 2\cos(2\pi/n)$ and for each such ρ there are $\beta \in \mathbb{Z}[\rho]$ following the definition 2.2.1. Each of these numbers β are associated with the same quasicrystals and so it is sufficient to only pick one representative.

Moreover since $2\cos(2\pi/5) = \frac{\sqrt{5}-1}{2} = \frac{\sqrt{5}+1}{2} - 1 = 2\cos(2\pi/10) - 1$ the extension rings $\mathbb{Z}[2\cos(2\pi/5)]$ and $\mathbb{Z}[2\cos(2\pi/10)]$ are identical and by extension the quasicrystals associated are also the same. Therefore we can skip the 5-fold rotational symmetry.

To summarize, quadratic Pisot-cyclotomic numbers β can only be associated to quasicrystals with 8-fold, 10-fold or 12-fold rotational symmetries. Table 2.1 shows a list of quadratic Pisot-cyclotomic numbers interesting for Quasicrystallography.

n	ρ	β	ζ
8	$2\cos\left(\frac{2\pi}{8}\right)$	$1+\sqrt{2}$	$e^{2i\pi/8}$
10	$2\cos\left(\frac{2\pi}{10}\right)$	$\frac{1+\sqrt{5}}{2}$	$e^{2i\pi/10}$
12	$2\cos\left(\frac{2\pi}{12}\right)$	$2+\sqrt{3}$	$e^{2i\pi/12}$

Table 2.1: Pisot-cyclotomic numbers of degree 2, of order n, associated to ρ.

Now we want to explore the connection between Galois isomorphisms of ζ and β. As we have shown here and in Section 1.3.3, for quadratic Pisot-cyclotomic β is the associated root of unity ζ of degree 4 and among its four Galois isomorphisms are two that do not change the real part of ζ. Consequently they also do not alter $\rho = \zeta + \bar{\zeta} = 2\Re(\zeta)$ and by extension neither they alter ρ's extension ring $\mathbb{Z}[\rho]$. By further extension the two Galois isomorphisms of ζ also do not change $\beta \in \mathbb{Z}[\beta] = \mathbb{Z}[\rho]$.

It turns out that the other two Galois isomorphisms of ζ do change β to its conjugate root β', these two are important for our model of the quasicrystal, which we will present in the next section.

2.3 Quasicrystal model

There certainly are many ways to acquire a set that follows the attributes listed in Section 2.1. We utilize the cut-and-project scheme described in Section 1.5.

Even though we showed the two dimensional quasicrystal as subset of $\mathbb{C}$ it is sometimes preferable to treat it as subset of $\mathbb{R}^2$; the two coordinates are of course real and imaginary parts. Further we will mark the complex variants with $^{\mathbb{C}}$.

Definition 2.3.1. Let $n \in \mathbb{N} \setminus \{2,3,4,6\}$. Let β be a quadratic Pisot-cyclotomic number of order n, associated to $\rho = 2\cos(2\pi/n)$ (and $\zeta = e^{2\pi i/n}$).
Further let $*^{\mathbb{C}}$ be a Galois isomorphism of ζ, such that $\beta^{*^{\mathbb{C}}} = \beta'$ and let the real variant $* : \mathbb{R}^2 \to \mathbb{R}^2$ be defined as $(x,y)^* = (\Re\big((x+iy)^{*^{\mathbb{C}}}\big), \Im\big((x+iy)^{*^{\mathbb{C}}}\big))$.
Let $v_1, v_2 \in \mathbb{R}^2$:

$$v_1 = (1,0) \quad \text{and} \quad v_2 = (\Re(\zeta), \Im(\zeta))$$

and for the complex variant $M^{\mathbb{C}} = \mathbb{Z}[\beta] + \mathbb{Z}[\beta]\,\zeta$ let the real variant be $M = \mathbb{Z}[\beta]\,v_1 + \mathbb{Z}[\beta]\,v_2$, similarly for $N^{\mathbb{C}} = \mathbb{Z}\left[\zeta^{*^{\mathbb{C}}}\right]$ let $N = \mathbb{Z}[\beta]\,v_1^* + \mathbb{Z}[\beta]\,v_2^*$.
Lastly let $\Omega \subset N$ be bounded with nonempty interior.
The **model of two dimensional quasicrystal linked to irrationality β and window Ω** is the set:

$$\Sigma(\Omega) = \{x \in M \mid x^* \in \Omega\}$$

⌟

So far the entire theses was purely abstract. To give you an example of what a quasicrystal might look like, there is the image 2.1 which shows finite section of a two dimensional quasicrystal with 8-fold rotational symmetry.

To validate our quasicrystal model we of course have to show that it follows the attributes from Section 2.1. However first we list few properties of our model which will help us show that.

- Inclusion property:
$$\Omega_1 \subset \Omega_2 \quad \Rightarrow \quad \Sigma(\Omega_1) \subset \Sigma(\Omega_2)$$
- Union property:
$$\Sigma(\Omega_1 \cup \Omega_2) \;=\; \Sigma(\Omega_1) \cup \Sigma(\Omega_2)$$
- Translation property:
$$\Sigma(\Omega + x^*) \quad = \quad \Sigma(\Omega) + x \qquad \text{for } x \in M$$
- Scaling property:
$$\Sigma(\beta\Omega) = \beta'\Sigma(\Omega)$$

And now to validate our model.

1. uniform discreteness:
$$\exists\, r_1 > 0,\ \forall z_1, z_2 \in \Lambda, z_1 \neq z_2 :\ |z_1 - z_2| > r_1$$
2. relative density:
$$\exists\, r_2 > 0,\ \forall z \in \mathbb{C} :\ B(z, r_2) \cap \Lambda \neq \emptyset$$
The result of the cut-and-project scheme is a Delone set if the window Ω is bounded with nonempty interior, which is how we defined it.

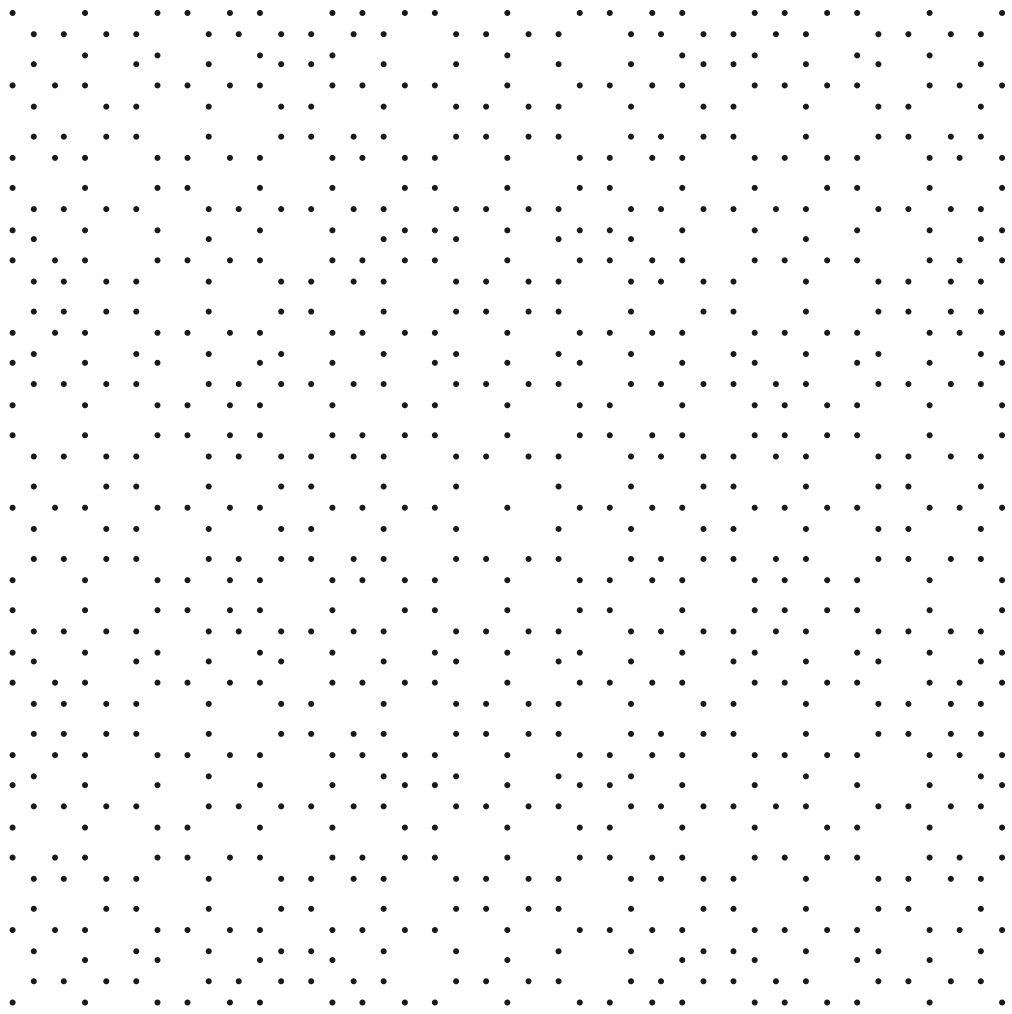

Figure 2.1: Example of a two dimensional quasicrystal.

3. finite local complexity:
$$\big|\{V(x) - x \,|\, x \in \Lambda\}\big| < \infty$$
It has been shown that our model has even this property, however since our work explores the list of Voronoi tiles we essentially prove this in the process.

4. rotational symmetry:
$$\exists\, \zeta = e^{2\pi i/n} : \ \zeta\Lambda^{\mathbb{C}} = \Lambda^{\mathbb{C}}$$
Rotational symmetry appears in quasicrystal if the window Ω has the same rotational symmetry.

5. dilation:
$$\exists\, b \in \mathbb{R} \setminus \{-1, 1\} : \ b\Lambda \subset \Lambda$$
Using the scaling property and the inclusion property:
$$\beta\Sigma(\Omega) = \Sigma(\beta'\Omega) \subset \Sigma(\Omega)$$

Having quasicrystal defined and our model validated, we shall present our plan for the analysis.

2.4 General quasicrystal analysis

In this section we will outline general method of analysis of any quasicrystal. Later we will use this method to analyze two dimensional quasicrystals.

Analysis should reveal the structure of the points of the quasicrystal, for us that means the list of Voronoi tiles for each quasicrystal.

To acquire such list we follow these steps:

1. **Acquire arbitrary finite section of the quasicrystal**

   In other words this means creating algorithm that for finite section $P \subset \mathbb{R}^d$ returns $P \cap \Sigma(\Omega)$.

2. **Estimate covering radius of the quasicrystal** R_C

   We are specifically interested in the upper bound $\hat{R}_C$ of the covering radius. This is necessary since on a Delone set Voronoi tile's domain's points can be no further from the center then double of the covering radius.

3. **Generate superset of all finite sections spanning** $B(2\hat{R}_C)$

   Each of these finite sections represents one Voronoi tile that appears in the quasicrystal's voronoi diagram.

4. **Filter the superset to the final list of Voronoi tiles**

   Due to technical constrains the previous step may have created more tiles than actually are in the list of Voronoi tiles and so it needs to be filtered.

These steps are general enough to analyze any quasicrystal associated with any Pisot-cyclotomic number and in any dimension. Unfortunately they are also too general and we will need to specify them for each quasicrystal.

We close this chapter and our general overview of quasicrystals with discussion of window shapes. It is obviously impossible to analyze a quasicrystal for arbitrary bounded $\Omega \subset N$ with nonempty interior. That is however not necessary. Not every two windows generate different quasicrystals, especially since we do not consider translated and/or β inflated quasicrystals to be different.

2.4.1 Analyzed window shapes

We will use the properties of quasicrystals to gradually limit the set of analyzed windows. We start with all of the windows:

$$\{\Omega \,|\, \Omega \subset N, \text{ bounded with nonempty interior}\}$$

To maintain our sanity we first limit our scope to convex bounded windows with nonempty interior.

$$\{\Omega \,|\, \Omega \subset N, \text{ convex bounded with nonempty interior}\}$$

Further thanks to the translation property we can limit our scope to convex bounded windows with nonempty interior centered around the origin:

$$\left\{\Omega - C_\Omega \,|\, \Omega \subset N, \text{ convex bounded with nonempty interior}\right\}$$

where C_Ω is the centroid or geometric center of the window Ω.

Lastly thanks to the scaling property we can limit our scope to convex bounded windows with nonempty interior centered around the origin of diameter in $(1/\beta, 1]$:

$$\left\{\Omega - C_\Omega, \,|\, \Omega \subset N, \; d(\Omega) \in (1/\beta, 1], \text{ convex bounded with nonempty interior}\right\}$$

where $d(\Omega)$ is the set diameter $d(\Omega) = \sup\{d(x, y) \,|\, x, y \in \Omega\}$, where $d(x, y)$ is the distance between x and y.

Remark. We could of course also pick any other β multiple of $(1/\beta, 1]$.

Of course even after all this limiting, the set of windows is still infinite. Therefore we will further limit our scope to three basic window shapes: rhombus, regular n-gon and a circle. The rhombus is not really a valid window since it is not sufficiently rotationally symmetrical, it is however fundamental to our method, more on this later. The regular n-gon represents the simplest window with sufficient rotational symmetry and the circle is interesting for its circular symmetry.

To summarize we will analyze quasicrystals for windows in shape of rhombus, regular n-gon and a circle centered around the origin of diameter in $(1/\beta, 1]$. Technically there is an infinite amount of these windows as well however as we will see later it is already manageable.

Finally we need to discuss the boundaries of the windows. Generally we will assume open windows i. e. we will exclude the boundary. The exception is the rhombus for reasons we will also explain later.

Now we have quasicrystal defined, model explored and windows limited. In the next chapter we will finally start the analysis.

Chapter 3

Analysis

The first step of analysis of the two dimensional quasicrystal is to create algorithm for acquiring arbitrary finite section of the quasicrystal. That is however not so simple. Luckily there is a workaround. Using specific window shape it is possible to decompose two dimensional quasicrystal into two quasicrystals with one dimensional windows. We will explain exactly what that means later, for now let's explore two dimensional quasicrystals with one dimensional windows.

By definition the quasicrystal with one dimensional window is a set of points whose star map images fit on a bounded section of a line. Since for a quasicrystal the star map inverse image of a line is again a line then two dimensional quasicrystal with a line segment for a window is in fact one dimensional (i.e. set of points on a line).

We present this connection between two dimensional and one dimensional quasicrystal mainly to avoid the need to explicitly define the attributes and show the properties of one dimensional quasicrystal. This way aside from the rotational symmetry all the attributes and all the properties apply to the one dimensional quasicrystal as well.

To summarize the motivation behind the analysis of one dimensional quasicrystal is the eventual analysis of two dimensional quasicrystal. To take full advantage of previous work we view one dimensional quasicrystal as a special case of two dimensional quasicrystal, that is two dimensional quasicrystal with a line segment for a window.

3.1 One dimensional quasicrystal

We can simplify our model for the specific case of one dimensional window. The easiest way is to position the window along the line $\{(x,0)|x \in \mathbb{R}\}$. That will result in a quasicrystal along the same line and thus we arrive to the following special case of the model of two dimensional quasicrystal:

Let β be a quadratic Pisot-cyclotomic number of order n, associated to $\rho = 2\cos(2\pi/n)$.
Further let $M = \mathbb{Z}[\beta]$ extension ring of β and $N = \mathbb{Z}[\beta']$ extension ring of β's conjugate root.
The projection $* : M \to N$ is the Galois isomorphism σ_1 (often denoted as $'$).
Lastly let $\Omega \subset N$ be bounded with nonempty interior.

Then the **model of one dimensional quasicrystal linked to irrationality β and win-**

dow Ω is the set:

$$\Sigma(\Omega) = \{x \in M \mid x^* \in \Omega\} = \left\{x \in \mathbb{Z}[\beta] \mid x' \in \Omega\right\}$$

Convex bounded one dimensional window is a line segment, which is in one dimension represented by an interval, specifically we will use left-closed right-open interval $\Omega = \left[-\frac{\ell}{2}, \frac{\ell}{2}\right)$ where $\ell \in (1/\beta, 1]$.

As we see in the following breakdown, quasicrystals with different openness or closeness differ only by at most a single point.

$$\Sigma((c,d)) = \begin{cases} \Sigma([c,d)) & c \notin \mathbb{Z}[\beta] \\ \Sigma([c,d)) \setminus \{c'\} & c \in \mathbb{Z}[\beta] \end{cases}$$

$$\Sigma([c,d]) = \begin{cases} \Sigma([c,d)) & d \notin \mathbb{Z}[\beta] \\ \Sigma([c,d)) \cup \{d'\} & d \in \mathbb{Z}[\beta] \end{cases}$$

$$\Sigma((c,d]) = \begin{cases} \Sigma((c,d)) & d \notin \mathbb{Z}[\beta] \\ \Sigma((c,d)) \cup \{d'\} & d \in \mathbb{Z}[\beta] \end{cases}$$

Unfortunately the addition or the removal of the single point causes occurrences of local configurations that appear only once in the entire quasicrystal. That would needlessly complicate our work and therefore we chose to only analyze left-closed right-open interval, which does not suffer from these zero density occurrences.

According to our plan, first step of the analysis is generating arbitrary finite section of one dimensional quasicrystal.

3.1.1 Arbitrary finite section

The picture 3.1 illustrates well, what we want to acquire – the sequence of points on the M axis. For this purpose we define the sequence of the quasicrystal.

Definition 3.1.1. Strictly increasing sequence $(y_n^\Omega)_{n\in\mathbb{Z}}$ defined as $\left\{y_n^\Omega \mid n \in \mathbb{Z}\right\} = \Sigma(\Omega)$ where $\Sigma(\Omega)$ is one dimensional quasicrystal is called the **sequence of the quasicrystal** $\Sigma(\Omega)$. ⌟

Now we would like to explore the set of all possible distances between two consecutive points of the sequence of the quasicrystal:

$$\left\{y_{n+1}^\Omega - y_n^\Omega \mid n \in \mathbb{N}\right\}$$

For that we need an expression for y_n^Ω. Let's start with the simplest window: $[-\frac{1}{2}, \frac{1}{2})$. The key here is the length of the window – i.e. 1. First we do a little algebraic exercise with the

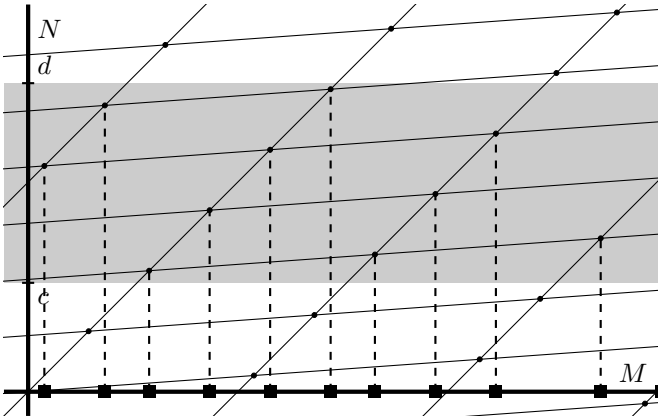

Figure 3.1: Illustration of one-dimensional quasicrystal. The grid is $M \times N$. On the N axis there is a window $\Omega = [c, d)$. The squares on the M axis are points of the quasicrystal $\Sigma(\Omega)$.

expression for the quasicrystal:

$$\begin{aligned}
\Sigma\left(\left[-\frac{1}{2}, \frac{1}{2}\right)\right) &= \left\{ x \in \mathbb{Z}[\beta] \;\middle|\; x' \in \left[-\frac{1}{2}, \frac{1}{2}\right) \right\} \\
&= \left\{ a + b\beta \;\middle|\; a + b\beta' \in \left[-\frac{1}{2}, \frac{1}{2}\right),\ a, b \in \mathbb{Z} \right\} \\
&= \left\{ a + b\beta \;\middle|\; -\frac{1}{2} \le a + b\beta' < \frac{1}{2},\ a, b \in \mathbb{Z} \right\} \\
&= \left\{ a + b\beta \;\middle|\; -\frac{1}{2} - b\beta' \le a < \frac{1}{2} - b\beta',\ a, b \in \mathbb{Z} \right\} \\
&= \left\{ \left\lceil -\frac{1}{2} - b\beta' \right\rceil + b\beta \;\middle|\; b \in \mathbb{Z} \right\}
\end{aligned}$$

Thus we can express the sequence of points of the quasicrystal as:

$$y_n^{\left[-\frac{1}{2}, \frac{1}{2}\right)} = \left\lceil -\frac{1}{2} - n\beta' \right\rceil + n\beta$$

And for the set of distances between two consecutive points we have:

$$\left\{ \left\lceil -\frac{1}{2} - (n+1)\beta' \right\rceil + (n+1)\beta - \left\lceil -\frac{1}{2} - n\beta' \right\rceil - n\beta \;\middle|\; n \in \mathbb{Z} \right\}$$

$$\left\{ \left\lceil -\frac{1}{2} - (n+1)\beta' \right\rceil - \left\lceil -\frac{1}{2} - n\beta' \right\rceil + \beta \;\middle|\; n \in \mathbb{Z} \right\}$$

$$\left\{ \left\lceil -\frac{1}{2} - n\beta' - \beta' \right\rceil - \left\lceil -\frac{1}{2} - n\beta' \right\rceil + \beta \;\middle|\; n \in \mathbb{Z} \right\}$$

Because β is Pisot we have $|\beta'| < 1$. Therefore the difference between the ceilings is either 0 or ± 1 (the sign depends on the sign of β') and the set of distances between two consecutive points

thus collapses to simple $\{\beta, \beta \pm 1\}$. We want to be clear that here ± 1 means either $+1$ or -1 depending on the sign of β', the set of distances between two consecutive points will have two members.

With a little thought and with use of the scaling property of a qusicrystal we can expand this to any window of size β^k where $k \in \mathbb{Z}$.

$$\Sigma\left(\beta\left[-\frac{1}{2}, \frac{1}{2}\right)\right) = \beta'\Sigma\left(\left[-\frac{1}{2}, \frac{1}{2}\right)\right)$$

Thus for window $\left[-\frac{\beta^k}{2}, \frac{\beta^k}{2}\right)$ we have the set of distances between two consecutive points $\left\{\left|(\beta')^k\beta\right|, \left|(\beta')^k(\beta \pm 1)\right|\right\}$.

Now we utilize the fact, that β is a quadratic integer – i.e. root of polynomial $x^2 + bx + c$ for $b, c \in \mathbb{Z}$. Thus we can use Vietas's formulas and also $\beta = -b - \frac{c}{\beta}$.

Applying Vieta's formula ($\beta' = \frac{c}{\beta}$) we have:

$$\left\{\left|\frac{c^k}{\beta^{k-1}}\right|, \left|\frac{c^k}{\beta^{k-1}} \pm \frac{c^k}{\beta^k}\right|\right\}$$

And applying $\frac{c}{\beta} = -\beta - b$ we get:

$$\left\{\left|(-1)^k\beta(\beta+b)^k\right|, \left|(-1)^k\beta(\beta+b)^k \pm (-1)^k(\beta+b)^k\right|\right\} = \left\{\left|\beta(\beta+b)^k\right|, \left|\beta(\beta+b)^k \pm (\beta+b)^k\right|\right\}$$

In the scope of our interest we now know the set of distances between two consecutive points for window of size 1: $\{\beta, \beta \pm 1\}$ and just outside of our scope for window of size $\frac{1}{\beta}$: $\left\{\left|\frac{b\beta}{c} + 1\right|, \left|\frac{b\beta \pm \beta}{c} + 1\right|\right\}$. Now we need to expand this knowledge to the entire interval $(\frac{1}{\beta}, 1]$.

It is possible to do this expansion for general quadratic Pisot-cyclotomic β, as for example in [**?**]. We analyzed each β individually, there however are several outcomes that apply generally and are important for further progress:

- there are two or three different distances between two consecutive points of a quasicrystal, often denoted from smallest to largest as S, M and L
- the distances vary with different window length
- the star map images of points of a quasicrystal that precede a certain distance form an interval

The last outcome is of particular importance for us. In essence it mean that there are one or two dividing points in the window of a quasicrystal that divide it into sections whose star map preimages precede the same distance in the quasicrystal. By extension it is also possible to divide the window by the distance that the points follow. We will explore this concept in greater detail later.

Based on these findings it is already possible to generate a finite section of a one dimensional quasicrystal.

- 0 is a fixed point of Galois isomorphism. 0 is also in every window centered around the origin (i.e. 0). Therefore 0 is present in every one dimensional quasicrystal with a window centered around it.

- We can acquire the next and previous points by identifying a section of a window the star map image of the point is present in and adding or subtracting appropriate distance.

For summary we outline the algorithm for acquiring arbitrary finite section of a one dimensional quasicrystal a bit more formally.

Input: window $[-\frac{\ell}{2}, \frac{\ell}{2})$; finite interval $[x_1, x_2]$

1. iterate through the points of the quasicrystal from 0 until you enter $[x_1, x_2]$
2. continue iterating while saving points in a list `quasicrystal` until you exit $[x_1, x_2]$

Output: the list `quasicrystal`

Thus we have accomplished the first step of our analysis. In the next section we will follow with the second step: estimating covering radius of the quasicrystal.

3.1.2 Estimate covering radius of the quasicrystal R_C

The estimation is rather straight forward in the one dimensional case, it will be more complicated for the two dimensional case and we do it here for sake of consistency.

Our definition of covering radius 1.1.2 simplified for one dimensional $D \subset \mathbb{R}$ would be:

$$R_C = \inf \{r_2 > 0 \,|\forall x \in \mathbb{R} :\ B(x, r_2) \cap D \neq \emptyset\}$$

So we are looking for the upper bound of the largest possible distance to the nearest point of the quasicrystal from anywhere on the number line.

As we have already found out in the previous section, there is a maximum distance between two consecutive points of the quasicrystal. Therefore the estimate we are looking for must be the half of the largest distance between two consecutive points.

$$\hat{R}_C = \frac{1}{2} \max_{n \in \mathbb{Z}} \{y^{\Omega}_{n+1} - y^{\Omega}_n\}$$

In the next section we will use this estimate to generate a superset of all finite sections spanning $B(2\hat{R}_C)$.

3.1.3 Generate superset of all finite sections spanning $B(2\hat{R}_C)$

We want to briefly get back to our over all goal and explain the motivation behind this step in greater detail.

Our goal is to acquire the list of Voronoi tiles in one dimensional quasicrystal. It is possibly quiet unusual to construct a Voronoi diagram on a one dimensional set. Once again we do it for consistency, however it also makes our presentation of results easier.

By Theorem 1.2.2 the domain of a Voronoi tile is limited by $B(x, 2\hat{R}_C)$ where x is the center of the tile. That is the motivation for this step.

Now let's continue with the exploration of one dimensional quasicrystal from two sections ago. We are going to create an algorithm that will for given $n \in \mathbb{N}$ and window Ω return a list of

finite sequences of $n+1$ points each that entail all possible centered $n+1$ points long sequences of consecutive points of the quasicrystal:

$$\left\{(y_i^\Omega - y_{i+\lfloor \frac{n}{2} \rfloor}^\Omega, y_{i+1}^\Omega - y_{i+\lfloor \frac{n}{2} \rfloor}^\Omega, \ldots, y_{i+n+1}^\Omega - y_{i+\lfloor \frac{n}{2} \rfloor}^\Omega) \mid i \in \mathbb{Z}\right\}$$

For that we introduce the notion of the stepping function of a quasicrystal.

Definition 3.1.2. Let $\Omega = [-\frac{\ell}{2}, \frac{\ell}{2})$ for $\ell \in \mathbb{Q}(\beta)$. The **stepping function** of the quasicrystal $\Sigma(\Omega)$ is the function $f^\Omega : \Omega \to \Omega$:

$$f^\Omega(y_n^{\Omega\prime}) = y_{n+1}^{\Omega\ \prime}$$

⌟

Remark. Note that the stepping function works with the star map images, not with the points of the quasicrystal.

The stepping function is a piecewise linear function. Each one of the two or three linear segments corresponds to one distance between the consecutive points of the quasicrystal. This aspect is what we are going to use for our algorithm. If we iterate the stepping function (i.e. $f^\Omega \circ f^\Omega$ or $(f^\Omega)^2$) we of course get again a piecewise linear function, this time with more discontinuities. The linear segments now correspond to pairs of the distances between two consecutive points of the quasicrystal. Not only that, there is a linear segment for each possible pair of the distances. There is an illustration of the concept in the Figure 3.2.

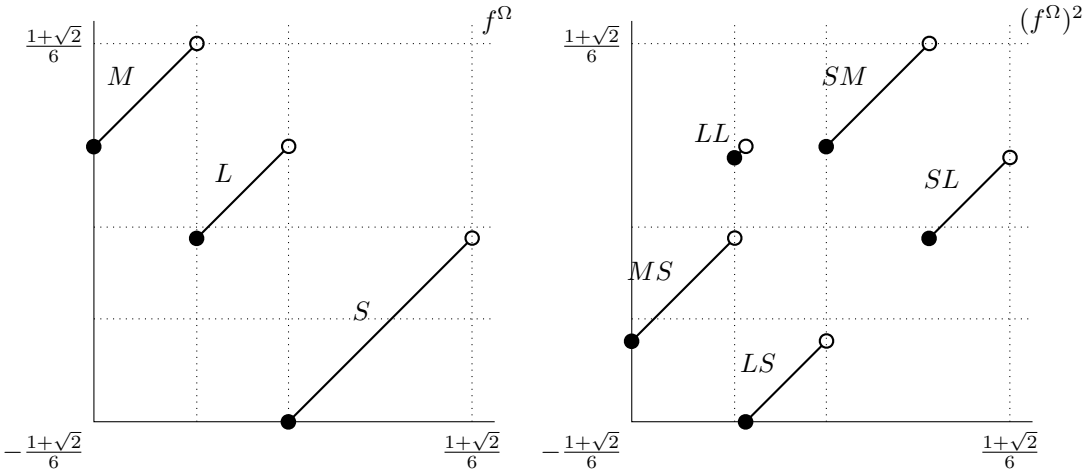

Figure 3.2: Example of the stepping function for for $\beta = 1+\sqrt{2}$ and window $\Omega = \left[-\frac{1+\sqrt{2}}{6}, \frac{1+\sqrt{2}}{6}\right)$. On the left there is just the stepping function and on the right there its second iteration. Letters S, M, L mark different lengths of distances.

Now the algorithm should be quite obvious. We are going to iterate the stepping function n times and from each finite sequence of the distances construct a finite section of $n+1$ points of the quasicrystal.

Again we summarize with a more detailed description of the algorithm.

Input: window $[-\frac{\ell}{2}, \frac{\ell}{2})$; number $n \in \mathbb{N}$

1. save the three linear segments of $f^{\Omega}(\Omega)$ as intervals in a list `segments`, mark each with the corresponding distance

2. repeat $n-1$ times: for each interval $I \in$ `segments` save the linear segments of $f^{\Omega}(I)$, append the marks accordingly

Output: list of marks of intervals from `segments`

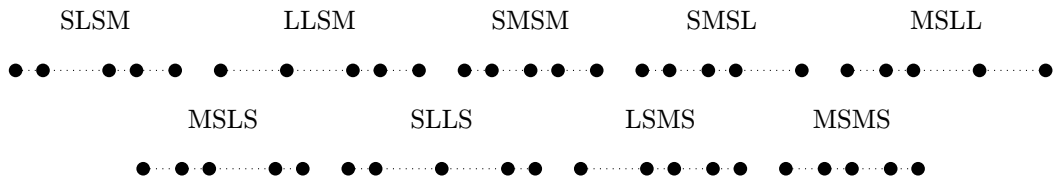

Figure 3.3: Example of the list of sequences of distances for $\beta = 1+\sqrt{2}$, $n = 4$ and window $\Omega = \left[-\frac{1+\sqrt{2}}{6}, \frac{1+\sqrt{2}}{6}\right)$. Letters S, M, L mark different lengths of distances. $S = \beta$, $M = \beta + 1$ and $L = 2\beta + 1$. Below each sequence of distances is the created finite section of the quasicrystal.

Once we acquire the list of sequences of distances, we easily convert them to sequences of points of quasicrystal. There is an example of the algorithm output and this conversion in the Figure 3.3. Now it remains to solve for n based on the covering radius estimate $\hat{R}_C$.

We want the finite sections to span $B(2\hat{R}_C)$, in other words we want the finite sections to be at least $4\hat{R}_C$ long. The obvious solution is to run the algorithm for $n = 1$ measure the shortest sequence and if it is shorter than $4\hat{R}_C$, increase n by 1, run the algorithm again and repeat until you acquire not only the n but also the list of the finite sequences of sufficient length.

It is also beneficial to choose an even n, that will result in odd number of points in the finite sections and that will ease the next step. Although it might result in the finite sections being longer than necessary.

Thus we have accomplished the third step of analysis and we can move on the next final step.

3.1.4 Filter the superset to the final list of Voronoi tiles

First we have to turn the list of finite sections from the previous step into a list of Voronoi tiles. Rather simply we just pick a point in each finite section as a center of the Voronoi tile. Here we see the benefit of having an odd number of points, since we can just pick the middle point. Constructing a Voronoi cell is then straight forward.

As we can see in the example in the Figure 3.4, several tiles appear multiple times, that is intrinsic to our method. Now we can simply select unique Voronoi tiles and present the tiles just with their domains (Figure 3.5).

It may seem that the analysis ends here, however even though it did not happen in our example it might happen that the acquired list of Voronoi tiles contains tiles that do not actually appear in the quasicrystal. And so we want to present a method for dealing with such eventuality.

For demonstration, let's add to our example list two more Voronoi tiles that we will eventually identify and remove (Figure 3.6). We will regard these added Voronoi tiles as artificial.

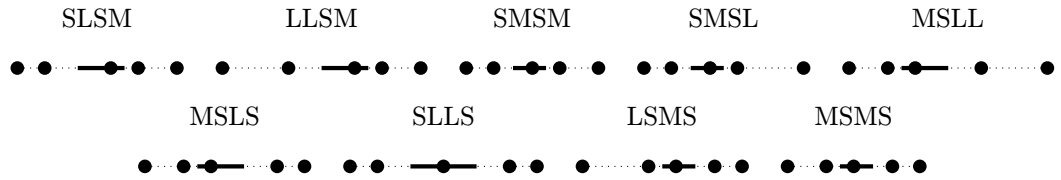

Figure 3.4: Example of the Voronois tiles on the list of finite sections of a quasicrystal for $\beta = 1 + \sqrt{2}$, $n = 4$ and window $\Omega = \left[-\frac{1+\sqrt{2}}{6}, \frac{1+\sqrt{2}}{6}\right)$. Voronoi tiles are represented by the thick line.

Figure 3.5: Example of unique Voronois tiles (from Figure 3.4) with their domains from a quasicrystal for $\beta = 1+\sqrt{2}$, $n = 4$ and window $\Omega = \left[-\frac{1+\sqrt{2}}{6}, \frac{1+\sqrt{2}}{6}\right)$. Voronoi tiles are represented by the thick line.

Figure 3.6: Example of the Voronois tiles with their domains from a quasicrystal for $\beta = 1 + \sqrt{2}$, $n = 4$ and window $\Omega = \left[-\frac{1+\sqrt{2}}{6}, \frac{1+\sqrt{2}}{6}\right)$ with **two extra** Voronoi tiles that do not appear in the quasicrystal.

Now we will explore the relationship between a Voronoi tile $V(x)$ and the window Ω of the quasicrystal. For the Voronoi tile to exist in the quasicrystal the star map images of its center x and domain $D(x)$ must fit inside the window Ω. Let's denote the points of the domain as $\{d_1, \ldots, d_k\} = D(x)$.

$$x^* \in \Omega \quad \wedge \quad d_i^* \in \Omega \quad \forall i \in \hat{k}$$

$$q_i = d_i - x \quad \forall i \in \hat{k}$$

$$x^* \in \Omega \quad \wedge \quad x^* + q_i^* \in \Omega \quad \forall i \in \hat{k}$$

$$x^* \in \Omega \quad \wedge \quad x^* \in \Omega - q_i^* \quad \forall i \in \hat{k}$$

$$x^* \in \bigcap_{i \in \hat{k}} (\Omega - q_i^*) \cap \Omega$$

This is very important, we have now turned the question whether a Voronoi tile could appear in the quasicrystal into the question whether an intersection of several translated windows is empty.

Now we can for each of the Voronoi tiles on our list construct such intersection and find out whether it is empty. It just happens that the section of the smallest Voronoi tile is empty (Figure 3.7).

Just for illustration we also show the intersection of one of the tiles that appears in the quasicrystal (Figure 3.8).

The second Voronoi tile we artificially added does however pass this filter. To get the final list of Voronoi tiles of the quasicrystal, we have to again look at the window.

Figure 3.7: Example of the elimination of a Voronoi tile by window intersection. This tile would be eliminated.

Figure 3.8: Example of the elimination of a Voronoi tile by window intersection. This tile would pass.

The intersection we used to eliminate some of the tiles does contain more information. A point of quasicrystal whose star map image fits in the intersection will be surrounded by the corresponding domain:

$$x \in \Sigma(\Omega) \quad \wedge \quad x^* \in \bigcap_{i \in \hat{k}} (\Omega - q_i^*) \cap \Omega \qquad \Rightarrow \qquad x + q_i \in \Sigma(\Omega) \quad \forall\, i \in \hat{k}$$

That however does not yet dictate the Voronoi tile that belongs to the point. The intersections for various Voronoi tiles may overlap. A point of quasicrystal whose star map image fits in multiple intersections will be surrounded by multiple domains and thus the resulting Voronoi tile will be the smallest one of the acceptable ones.

We illustrate this process with two figures. Figure 3.9 shows a list of Voronoi tiles with corresponding window intersections. Note that the intersections do overlap.

Figure 3.10 shows that the smallest tile will indeed be the one that appears in the quasicrystal.

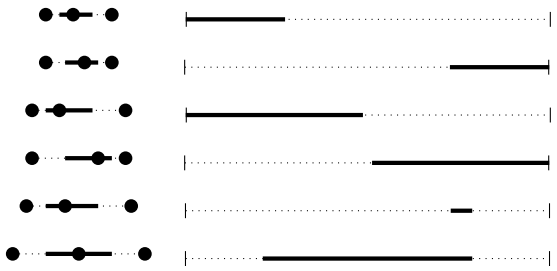

Figure 3.9: List of Voronoi tiles with corresponding window intersections. The tiles are sorted from top to bottom by increasing size.

Figure 3.10: A window of a quasicrystal divided by overlapping intersections from Figure 3.9. Voronoi tile above each section shows which Voronoi tile would appear in the quasicrystal.

We can also see that the second artificially added Voronoi tile does not pass this filter since it is bigger than another Voronoi tile whose intersection is a superset of the intersection of the artificial Voronoi tile. It could also happen that its intersection would be covered by multiple intersections of smaller Voronoi tiles. In this context covered means that for each point in the

intersection of the artificial Voronoi tile there is an intersections of smaller Voronoi tile that also contains said point.

All together this last step of the analysis consists of three filters:

1. Eliminate duplicate Voronoi tiles.
2. Eliminate Voronoi tiles whose intersection $\bigcap_{i \in \hat{k}} (\Omega - q_i^*) \cap \Omega$ is empty.
3. Eliminate Voronoi tiles whose intersection $\bigcap_{i \in \hat{k}} (\Omega - q_i^*) \cap \Omega$ is covered by intersections of other smaller Voronoi tiles.

Corollary

Figure 3.10 suggests that we could divide the window of a quasicrystal into sections corresponding to different Voronoi tiles. That is in fact possible and is a nice tool for presenting results.

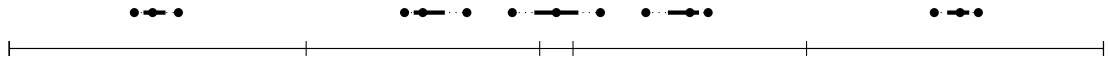

Figure 3.11: A window of a quasicrystal divided into sections corresponding to different Voronoi tiles.